

# UC Irvine

## UC Irvine Previously Published Works

### Title

Technical Advances and Applications of Spatial Transcriptomics.

### Permalink

<https://escholarship.org/uc/item/8k94026m>

### Journal

GEN Biotechnology, 2(5)

### Authors

Liang, Guohao

Yin, Hong

Ding, Fangyuan

### Publication Date

2023-10-01

### DOI

10.1089/genbio.2023.0032

Peer reviewed



Published in final edited form as:

*GEN Biotechnol.* 2023 October ; 2(5): 384–398. doi:10.1089/genbio.2023.0032.

## Technical Advances and Applications of Spatial Transcriptomics

Guohao Liang<sup>1,†</sup>, Hong Yin<sup>1,†</sup>, Fangyuan Ding<sup>2,\*</sup>

<sup>1</sup>Department of Biomedical Engineering, University of California, Irvine, Irvine, California, USA.

<sup>2</sup>Center for Synthetic Biology, Center for Complex Biological Systems, Department of Developmental and Cell Biology, and Department of Pharmaceutical Sciences, University of California, Irvine, California, USA.

### Abstract

Transcriptomics is one of the largest areas of research in biological sciences. Aside from RNA expression levels, the significance of RNA spatial context has also been unveiled in the recent decade, playing a critical role in diverse biological processes, from subcellular kinetic regulation to cell communication, from tissue architecture to tumor microenvironment, and more. To systematically unravel the positional patterns of RNA molecules across subcellular, cellular, and tissue levels, spatial transcriptomics techniques have emerged and rapidly became an irreplaceable tool set. Herein, we review and compare current spatial transcriptomics techniques on their methods, advantages, and limitations, as well as applications across a wide range of biological investigations. This review serves as a comprehensive guide to spatial transcriptomics for researchers interested in adopting this powerful suite of technologies.

---

RNA is one of the most important families of molecules in biology, functioning at almost every level of cellular processes.<sup>1</sup> As a median between genetic material and protein products, production and modulation of messenger RNA is crucial for organism functioning, with its mis-regulation leading to many diseases.<sup>2–7</sup> Besides, noncoding RNA,<sup>8,9</sup> small RNA,<sup>10,11</sup> and other functional RNA<sup>12</sup> intricately regulate gene expression pathways in transcription,<sup>13,14</sup> RNA processing,<sup>15,16</sup> and translation.<sup>17,18</sup>

Transcriptomics studies the complete set of RNA transcripts that are produced by cells within specific physiological conditions or cell types. It is crucial for understanding the identity of cells, their function within the respective tissue context, and their changes throughout the course of disease development.<sup>19–22</sup> Over the past decade of transcriptomics, RNA sequencing, especially single-cell RNA sequencing (scRNA-seq), has been the main workhorse and provided vast knowledge on the transcriptome in many settings, including cancer,<sup>23,24</sup> embryo development,<sup>25,26</sup> immunology,<sup>27,28</sup> tissue profiling<sup>29–31</sup> and more.

---

\* Address correspondence to: Fangyuan Ding, Biomedical Engineering, University of California, Irvine, Room 4400 ISEB Building, Irvine, CA 92617, USA, dingfy@uci.edu.

† Co-first authors

Authors' Contributions

G.L. and H.Y. contributed equally and are listed alphabetically. All authors have given substantial input into writing original draft and writing review and editing.

Author Disclosure Statement

No competing financial interests exist.

Spatial transcriptomics have emerged over recent years to complement scRNA-seq, in that it specifically addresses the challenge of retaining spatial contexts of RNA transcripts. It has quickly become an invaluable asset in transcriptomics that *Nature Methods* named spatial transcriptomics “Method of the Year 2020.”<sup>32</sup> The spatial context of RNA transcripts is important to study at multiple levels. At a tissue level, the relative positions of cells within their tissue contexts provide information on their identity, communication, and ultimately the function of tissues. For example, tumor microenvironment plays an important role in cancer growth and therapeutic response.<sup>33</sup> It contains subpopulations of cancer cells that differ from but interact with each other to constitute the tumor. To fully understand such intratumor cellular interactions, the relative spatial context between cell populations must be preserved. At a finer level, subcellular localization of RNA transcripts has been shown to affect cellular architecture and function.<sup>34,35</sup> In addition, subcellular localization can also be used to model RNA velocity,<sup>36,37</sup> which describes the integrated dynamics of RNA synthesis, nuclear export, cytoplasm translocation, and degradation.

Due to the broad impact of spatial transcriptomics studies, significant expansion of spatial transcriptomics technique development appears. These techniques achieve RNA spatial mapping by integrating various modern molecular biology techniques, including but not limited to fluorescent *in situ* hybridization (FISH),<sup>38,39</sup> next-generation sequencing (NGS).<sup>40</sup> Depending on the methodology adopted, spatial transcriptomics methods obtain different levels of spatial resolution, detection throughput, efficiency, and sensitivity (Table 1). For example, the commercially available Visium technology by 10X Genomics utilizes positional molecular barcodes to maintain spatial context of tissue ahead of RNA sequencing, which enables transcriptome-wide coverage.<sup>41</sup> Another recently commercialized technology, Multiplexed Error-Robust Fluorescence *in situ* Hybridization (MERFISH),<sup>42–45</sup> relies on sequential single-molecule FISH that allows for single-cell resolution with near 100% detection efficiency.

In this review, we introduce the technical advancement of spatial transcriptomics over the years and demonstrate the capabilities of spatial transcriptomics in a variety of biological investigations. We aim to provide a guide for researchers that are looking to adopt spatial transcriptomics in their research to selecting different spatial transcriptomics strategies.

## Spatial Transcriptomics: Techniques

Spatial transcriptomics techniques can be broadly categorized into three major groups: hybridization-based methods, *in situ* sequencing-based methods, and *ex situ* sequencing-based methods (Fig. 1). In the hybridization-based methods, spatial RNA patterns are determined by mapping RNA molecules through hybridization with fluorescent complementary probes. *In situ* sequencing-based methods, on the other hand, involve sequencing RNA molecules directly within intact tissue sections. *Ex situ* sequencing-based methods, which also involve sequencing, barcoding, and capturing RNA molecules from spatially defined regions of the tissue after physically isolating them. In the following, we will elaborate all three categories and compare their advantages as well as disadvantages. A summarized version is in Table 1.

## Hybridization-based methods

Hybridization-based methods map RNA molecules with spatial locations by the hybridization between fluorophore-labeled DNA probes and the RNA targets. Depending on the specific probe designs, these techniques can be classified into three groups, with single molecule detection, high-sensitive detection, as well as multiplexing as purposes.

**Single molecule detection.**—Single molecule detection methods aim to map single RNA molecules in the cell context. The first version, FISH, was developed by the Singer Lab in 1998 based on the RNA *in situ* hybridization (RNA-ISH) technique. In this early FISH technique, a set of ten DNA probes, each labeled with five fluorophores, are used to target RNA by complementary basepairing.<sup>39</sup> Compared to previous RNA-ISH, FISH substitutes the need of using a secondary dye or hazardous radioactive nucleotide for detection with fluorescence detection. The diversity of fluorescence colors enables measurement of multiple different RNA at the same time. The collective binding between the set of probes and the target RNA forms dots with strong fluorescent intensity in the cell. The number and intensity of dots reveal the quantity and spatial distribution of RNAs inside the cell at the moment of fixation.

Single-molecule FISH (smFISH) was then developed based on FISH. Singly labeled probes are used instead of multiple-labeled probes. A set of more than 20 probes is designed to target one RNA region.<sup>38</sup> The use of singly labeled probes circumvents the problem of probe heterogeneity due to the inconsistent labeling efficiency in multilabeled probes. These changes achieve a higher signal-to-noise ratio. Further optimization and specialization were done based on smFISH. For instance, TurboFISH developed multiple fixations, permeabilization, and hybridization conditions to reduce the probe hybridization time to several hours.<sup>46</sup>

Beyond single molecule detection, single nucleotide variant (SNV) has also been identified spatially. For instance, a toehold probe labeled with a fluorophore can be used together with a set of smFISH probe to identify SNVs.<sup>47</sup> inoFISH modified the targeting sequence in the toehold probe to suit the need for detecting adenosine-to-inosine base editing.<sup>48</sup> Worth mentioning, despite that these toehold probe methods are capable of detecting SNVs, the detection efficiency remains low, due to the weak fluorescent signal from singly labeled toehold probe, as well as the limited accessibility of target RNA single-binding site.

**High-sensitive detection.**—High-sensitive detection methods aim to map RNA molecules in large tissue samples with high-background noise. Visualizing RNA in large tissue sample has been challenging. First, tissue sample is often auto-fluorescent and opaque, thus hard to achieve a good signal-to-noise ratio using smFISH. In addition, RNA molecules, especially the lowly expressed transcripts, are difficult to be identified in large tissue samples; therefore, signal amplification is desired. In the following, we will compare three high-sensitive detection methods developed in recent 10 years.

Hybridization chain reaction (HCR) is one of the signal amplification methods developed in the early 2000s. In HCR, the binding of probes on the RNA target leads to the iterative binding of two types of fluorescence hairpins, where the extension of hairpin chain

results in stronger fluorescent signal.<sup>49</sup> Then, to reduce the cost of redesigning expensive fluorescent hairpins for different RNA targets, HCR v2.0<sup>50</sup> introduces a primary probe to bridge the hairpin chain to RNA target, achieving an RNA target independent library of fluorescent hairpins. HCR v3.0 further optimizes the architecture by using a pair of split oligonucleotides to bridge the RNA target and primary probe,<sup>51</sup> which reduces the nonspecific binding.

One major benefit of HCR is its strong fluorescent signal to visualize RNA at low magnification objectives, even under flow cytometry.<sup>51,52</sup> The design of HCR is thus also adopted by other amplification-based techniques. For instance, ultrasensitive sequential FISH (UseqFISH) combines rolling-circle amplification (RCA) and HCR to achieve even higher amplification to detect adeno-associated viruses transduction by targeting short viral RNAs.<sup>53</sup> Additionally, high-fidelity amplified FISH (amp-FISH) combines HCR and a pair of split hairpins to detect SNV.<sup>54</sup>

Similar to HCR's split-oligonucleotides design, RNAScope<sup>55</sup> uses a pair of Z-shaped probes to bridge the RNA target and the amplification region. Instead of the iterative binding between two fluorescent hairpins like HCR, RNAScope utilizes a preamplifier to form scaffolds for the binding of the fluorescent amplifier oligonucleotides. Compared to HCR, the use of the scaffold allows better control of the scale of signal amplification.

Another recently developed method is Click-amplifying FISH (Clamp-FISH). Specifically, Clamp-FISH<sup>56</sup> hybridized a primary padlock-probe on its RNA target, then locked them by applying click chemistry between the terminal alkyne and azide on the padlock-probe. Then, sets of amplification padlock-probes with fluorophores are hybridized upon the primary probe and locked through similar click chemistry. To reduce the cost of probe synthesis by pooled synthesis, ClampFISH 2.0 modified the padlock probe structure by internalizing the targeting sequence.<sup>57</sup> The redesign of the amplification padlock probe allows multiplexing with ten RNA species and compatibility with tissue sections. The extent of amplification in ClampFISH can be controlled by the number of rounds of hybridization and clicking chemistry. Locking probes by click chemistry allows stringent washes to reduce nonspecific binding without worrying washing away the truly bound probes.

Despite many remarkable advantages of high-sensitive detection, current amplification-based methods exhibit some limitations too. Along with amplification on the true RNA targets, nonspecific signals are also amplified. Although this can be alleviated using split oligonucleotide pairs, such a nonspecific amplification problem is not fully resolved. Additionally, the extent of amplification on RNA is heterogeneous, as amplification can only be controlled at broad level but not at single molecule level, leading to bias in RNA transcript quantification. Furthermore, excessive amplification increases optical crowding, merging of which signals from multiple targets, result in the missing of single-molecule signals.

**Multiplexing.**—Multiplexing methods aim to map RNA expressed from thousands of genes in the whole transcriptome. Previously mentioned methods, such as smFISH, can only multiplex through the usage of distinguishable fluorescent channels, but with limited

diversity of fluorophores, whole spatial transcriptomics mapping becomes impractical. Thus, highly multiplexable methods are needed and then achieved by adopting barcoding schemes. In the following, we will introduce two widely used barcoding methods: sequential fluorescence *in situ* hybridization (seqFISH) and MERFISH, both dramatically increases the multiplexability of hybridization-based spatial transcriptomics methods.

seqFISH barcodes the RNA targets through the fluorescent signals on the same RNA targets in multiple rounds of probe hybridization.<sup>58</sup> In details, seqFISH targets the same RNA targets at the same regions in multiple rounds using the same set of smFISH probes conjugated with different fluorophores. After a round of imaging readout, the hybridized probes are stripped away from their RNA partners by high percentage formamide buffer and are digested by DNase, leaving the RNA targeting site open for the next round of hybridization. The alignment of fluorescent signals from multiple rounds of hybridization results in color barcodes for every RNA target. The number of barcodes scales up exponentially with number of sequential hybridizations. For instance, seqFISH has achieved to map 249 genes in the mouse hippocampus transcriptome,<sup>59,60</sup> and can also be modified to detect multiple genomic loci in combination with CRISPR-Cas9 system.<sup>61</sup>

In the ameliorated version of seqFISH+,<sup>62</sup> the improvement of barcoding strategy and the design of the seqFISH+ probes achieve a much higher barcoding capacity. Specifically, SeqFISH performs barcoding through sequential hybridization, effectively creating 60 pseudocolors split into three fluorescence channels. Noticeably, these pseudocolors are not based on color but on the presence of sequentially hybridized probes in each of the 20 hybridization cycles within one round. Subsequently, four rounds of seqFISH+ will generate a unique four-unit barcode readout based on the 20 hybridization signals in each round.<sup>62</sup> The most similar three out of the four units within the readout are used to align barcodes to their gene identities. This error correction scheme tolerates the absence or misread of one signal readout.<sup>60,62</sup> By employing the 20 pseudocolors in each channel, SeqFISH+ effectively dilute the portion of RNA to be imaged at each hybridization by 20-fold, reducing the optical density to its one 20th while enlarging the barcode capacity to 8,000 per channel.<sup>62</sup> With such a high barcoding capacity, seqFISH+ can multiplex 10,000 genes in the tissue sample.<sup>62</sup>

On the other hand, MERFISH, which also relies on sequential hybridization, utilizes a different probe design and a unique barcoding scheme. The sequential targeting of the readout sites by fluorescent readout probes at each round, followed by cleavage of disulfide bonds between readout probes and fluorophores, generates barcodes for each RNA target.<sup>43,44</sup> Unlike seqFISH+ barcoding, MERFISH uses a Hamming distance coding approach to enhance robustness. Specifically, MERFISH constructs the binary codes with constant hamming weight of 4 and with hamming distance of either 2 or 4.<sup>43,44</sup> The utilization of hamming distance in the barcodes makes MERFISH error robust: it takes at least two or four misread in the fluorescence signal readout to be misidentified as another barcodes.<sup>43,44</sup> In the recent work, MERFISH has successfully mapped 10,000 genes in the tissue sample.<sup>63</sup>

Despite fascinating multiplexing ability, current multiplexable hybridization techniques have mild drawbacks. In particular, sample autofluorescence and optical crowding, arising from fluorescent probes binding on a large amount of RNAs at the same time, can impact the barcoding stringency because they interfere with the alignment of fluorescence signals from sequential rounds of hybridization. In addition, the specificity could also be affected if fluorescent probes from previous hybridization is not thoroughly washed away. Worth mentioning, both of seqFISH+ and MERFISH adopt different strategies to alleviate these drawbacks. SeqFISH+ increases the total number of hybridizations by employing the pseudocolor concept, effectively diluting the RNA fluorescent signals during each hybridization.<sup>62</sup> It also embeds all RNA onto hydrogel matrix and clears the tissue to reduce autofluorescence.<sup>62</sup> MERFISH, on the other hand, with fewer total numbers of hybridizations, embeds the polyadenylated RNA onto an expandable hydrogel matrix, with subsequent tissue clearing<sup>64</sup> and physical expansion,<sup>63</sup> to achieve high signal-to-noise ratio.

When designing experiment with SeqFISH+ and MERFISH, researchers should consider the balance between the barcode library size and stringency. In SeqFISH+, the barcode library size can be expanded by utilizing more fluorescence channels or increasing imaging rounds.<sup>60,62</sup> In MERFISH, although MHD4 barcodes is more stringent and robust than MHD2's, MHD4 encodes a much small library than MHD2, as 16bitMHD4 covers 140 genes, while 14bitMHD2 encodes 1001 genes.<sup>43,44</sup> For both seqFISH+ and MERFISH, more hybridizations will increase the barcode library size, but at the expense of longer experimental time in the serial hybridization and imaging and data processing. Therefore, a balance must be held between the stringency and library size to fit the actual needs in the research.

### ***In situ* sequencing-based methods**

Although hybridization-based spatial transcriptomics techniques are excellent tools to map RNA targets and the transcriptome, they have difficulty to distinguish nucleotide differences in RNA sequences or study the transcriptome without prior knowledge of RNA sequences. *In situ* sequencing techniques compensate these technical gaps. Specifically, they offer the tool for studying spatial transcriptomics at high base resolution at the intact cellular context, through either sequencing the transcriptome or multiplexing the barcodes by single-base resolution detection, with or without prior knowledge of RNA target sequences.

Fluorescent *in situ* sequencing (FISSEQ) is one of the earliest *in situ* sequencing methods. It incorporates primers to RNA targets *in situ*, reverse-transcribes RNA into cDNA, circularizes cDNA, and amplifies cDNA with RCA.<sup>65</sup> The amplicons are subjected to sequence-by-ligation with fluorescent oligonucleotides to interrogate the dinucleotides next to the sequencing primer. A total of four sets of sequencing primers with one-base frame-shifting are used to cover all base within the 30-base sequencing read.<sup>65</sup> With its powerful *in situ* sequencing ability, FISSEQ generates ~8,000 sequencing reads, corresponding to ~700 mRNAs on 40 cells.<sup>65</sup>

Barcode *in situ* targeted sequencing (BaristaSeq) utilizes a different targeting and sequencing design than FISSEQ. In particular, to increase detection efficiency, BaristaSeq targets RNA with gapped padlock probes and fills the gap with reverse transcription to



generate circular templates for RCA.<sup>66</sup> BaristaSeq also adapts the Illumina sequencing-by-synthesis method to sequence transcriptome with fluorescence nucleotide analogs in Illumina NGS chemistry.<sup>66</sup> This approach reduces the background noise arising from the fluorescent oligonucleotides that binds nonspecifically. With all these ameliorations, BaristaSeq achieves a sequencing accuracy as high as 97%.

In recent years, hydrogel embedding and tissue clearing have also been integrated into *in situ* sequencing by spatially resolved transcript amplicon readout mapping (STARmap)<sup>67</sup> and expansion sequencing (ExSeq).<sup>68</sup> Specifically, STARmap incorporates hydrogel embedding and tissue clearing by CLARITY<sup>69</sup> to reduce tissue auto-fluorescence and improve enzyme entry for sequencing. Additionally, the substitution of a single-padlock design with a SNAIL probe<sup>67</sup> containing five-base barcode helps bypass the reverse-transcription to increase targeting specificity and detection efficiency. STARmap achieves successful mapping of up to 1,024 gene in the tissue sample.<sup>67</sup> The image time is also greatly reduced to only six imaging cycles. However, because the barcodes are pre-integrated into the SNAIL probes, STARmap can only perform *in situ* sequencing with prior knowledge of the RNA targets.

On the other hand, ExSeq, which involves the hydrogel embedding with different chemistry formula, is able to physically expand the embedding sample<sup>68</sup> to achieve higher spatial resolution and lower optical crowding. With similar untargeting scheme in FISSEQ, ExSeq maps 326 genes in the neuronal tissues and 3039 genes in the tissue with 10 times volume.<sup>68</sup> Using the padlock probe barcoding scheme, ExSeq achieves a proof-of-principle mapping of 42 selected genes in-depth with more than 250,000 reads.<sup>68</sup>

This diverse set of *in situ* sequencing tools provides opportunities for researchers to study spatial transcriptomics in cells and tissue with single-base resolution and high multiplexity. Despite advantages, a few limitations still need to be addressed. For instance, the untargeted detection efficiency is low due to the low cDNA conversion rate. This could result in missing rare RNA species. A long turnover time, for example, a week or two in FISSEQ, prevents more extensive applications of the methods. In addition, in method without tissue clearing, autofluorescence and optical crowding may affect the sequencing readout.

### ***Ex situ* sequencing-based methods**

Although *in situ* sequencing can map RNA transcripts and the transcriptome with high multiplexity, it can miss transcript information due to its short read-length (~35 bases). *Ex situ* sequencing, on the other hand, use highly standardized and powerful NGS to reach a much longer read length, often >100 bases. Because sequencing takes place outside of the cells, each RNA transcripts must be barcoded to retain its spatial location before conversion to cDNA for NGS *ex situ*, so that the NGS reads, which contain information about both RNA identities and spatial locations, can then be decoded to reconstruct spatial transcriptomics profiles. In general, the *ex situ* sequencing-based methods can be classified into two groups based on the how spatial barcodes are incorporated into RNA *in situ*. We will elaborate each group in the following.

RNA *in situ* capturing by spatially barcoded oligonucleotides. This group barcodes RNA molecules by capturing RNAs via spatially barcoded oligonucleotides, after releasing RNA



transcripts from the sample. In details, the tissue sample is placed on a capturing slide coated with spatially distinct barcoded oligonucleotides containing a poly-(dT) region. Then the sample is digested, and the released mRNAs are captured by the barcoded oligonucleotides *in situ*. The converted cDNAs, which include both mRNA sequences and barcode sequences, are then amplified, pooled, and sequenced *ex situ*. Spatial transcriptomics profile is reconstructed based on the decoded sequencing reads.

XYZeq<sup>70</sup> is one of these methods compatible for tissue-level spatial transcriptomics studies. The capturing slide used in XYZeq contains microwell arrays, center-to-center distance of which is 500  $\mu\text{m}$  and coated with spatially distinct barcode oligonucleotides. Although its resolution is low, it has high capturing efficiency, making it suitable for tissue-level studies rather than cellular- or subcellular-level studies.

On the other hand, Slide-seq<sup>71</sup> and high-definition spatial transcriptomics (HDST)<sup>72</sup> are compatible with cell-level spatial transcriptomics studies. Slide-seq captures mRNA released from the cryo-preserved samples with 10  $\mu\text{m}$  beads with barcodes.<sup>71</sup> Slide-seqV2 further optimizes barcoding scheme and enzymatic preparation protocol from Slide-seq to increase the capturing efficiency.<sup>73</sup> With this high capturing and detecting efficiency, Slide-seqV2 can faithfully detect ~44% mRNA transcripts as in Drop-seq and identified more than 1,300 spatially differentially expressed genes in mouse developing neocortex.<sup>73</sup> HDST<sup>72</sup> captures mRNA released from the cryo-preserved sample with barcoded beads in 2  $\mu\text{m}$  microwells. The spatial location of these beads is decoded by multiple rounds of hybridization and imaging to obtain spatial information before cDNA pooling and sequencing. More than half of the cells in the mouse brain section have been successfully assigned into single cell type by HDST, proofing that its practical resolution reaches single cell level.<sup>72</sup> Though Slide-seq V2 and HDST achieve near single-cell resolution, experts and users in field concern the difficulties in making these small beads coated with barcoded oligos.

Slide-seq and HDST each have its unique advantages. For instance, although Slide-seqV2 has lower resolution, it has higher capturing rate than HDST. HDST, on the other hand, has higher resolution, and its capturing rate is between Slide-seq and Slide-seqV2. HDST is more time-consuming because it requires the several rounds of hybridization and imaging for barcode decoding before mRNA capturing. But other omics (like protein staining and H&E staining) can be included at this step if needed. Recently, SlideSeq-V2 has been commercially available, renamed as Curio Seeker, from Curio Bioscience.<sup>74</sup> Curio Seeker spatial mapping kit consists of a 3×3 mm capturing area, which is coated with a monolayer of 10  $\mu\text{m}$  capturing beads. The entire workflow from tissue sectioning to sequencing requires 8 h with the highly standardized protocol. Curio Seeker has been applied to map reovirus-induced myocarditis in neonatal mouse hearts to elucidate the pathogenesis of viral myocarditis.<sup>75</sup>

To achieve an even higher resolution, spatial enhanced resolution omics-sequencing (Stereo-seq) replaces microwells by 200 nm DNA nanoball array with 500 or 715 nm center-to-center distance to capture mRNA, enabling its use in cellular and subcellular studies.<sup>76</sup> Beside high-spatial resolution, Stereo-seq offers the capturing chip with 13.2×13.2 cm capturing area, which accommodates tissue samples with large sizes. With large capturing

area and high resolution, Stereo-seq generated detail spatial transcriptomics profiles for E16.5 mouse embryonic tissue samples, on average identifying the spatial expression of 529 genes per cell.<sup>76</sup> Stereo-seq has recently become available from STOmics.<sup>77</sup> The standard capturing area is 1×1 cm on the STOmics chip, and it can be customized to larger size up to 13×13 cm. The standardized protocol of Stereo-seq capturing and library construction requires roughly 1.5 days. Stereo-seq from STOmics has been used to map the axolotl brain regeneration to discover the functions of induced progenitor cells in such regeneration process.<sup>78</sup>

10X Visium is another commercially available kit for RNA capturing.<sup>79</sup> 10X Visium provides kits with two options, containing either four 6.5×6.5 mm or two 11×11 mm capturing areas, suitable for both fresh frozen and formalin-fixed paraffin-embedded samples. Each area is coated with spatially barcoded capturing probes to capture RNA. The captured RNA is barcoded and converted to cDNA, followed by sequencing to detect the RNA identities and spatial locations. The spatial resolution is at 10 cells level, meaning that Visium is suitable for board patterning of RNA expression in tissue samples. One of the benefits of using this commercially available kit is that it offers highly standardized experiment pipeline for the spatial transcriptomics studies. It can also combine with H&E staining and protein co-detection for multi-omic studies.

Despite the convenience of usage and their effective profiling by sequencing, the *ex situ* methods have a few limitations. For instance, lateral diffusion<sup>71,73,76,80</sup> of RNA transcript occurs during the RNA capturing, leading to slight changes in spatial gene expression patterns. Also, overlapping cells are not distinguished well because the capturing is in two-dimension. In addition, the release of RNA transcripts requires destroying the samples, preventing further handling on the sample after spatial transcriptomics analysis.

RNA *in situ* barcoding by spatially barcoded oligonucleotides. Instead of releasing RNAs first, this group barcodes RNA molecules by incorporating spatially barcoded oligonucleotides onto RNA inside cells. In particular, spatially barcoded oligonucleotides are delivered into fixed cells and directly hybridized with RNA transcripts *in situ*. The afterward sequencing and decoding steps are comparable to the previous section. We will specifically discuss three example methods in details.

Deterministic barcoding in tissue for spatial omics sequencing (DBiT-seq) utilize channels in the microfluidic chamber to deliver barcoded DNA poly-(dT) oligonucleotides to tissue sample spatially.<sup>81</sup> This method achieved 10 μm spatial resolution and high capturing rate of roughly 1–2 orders of magnitude as SlideSeq. Besides, DBiT-seq benefits from its ability to combine with protein detection by delivering barcoded antibodies. DBiT-seq has achieved the co-mapping of the mouse embryonic transcriptome with a set of 22 proteins,<sup>81</sup> and more than 2,000 genes have been captured and profiled in 10 μm pixel area.<sup>81</sup> Recently, DBiT-seq was further modified to make it compatible with ATAC-seq and CUT&Tag-seq on the same microfluidic chamber.<sup>82</sup> This improvement allows the co-mapping of spatial epigenomics and spatial transcriptomics. One of the limitations is that the capturing area is small (1 · 1 mm), necessitating the large number of capturing chambers to analyze large tissue samples.

Alternatively, light-seq<sup>83</sup> adopts the *in situ* barcoding through light-directed technique, with subcellular resolution. Specifically, barcoded oligonucleotides are iteratively added to the entire sample. By applying UV illumination in the region of interest (ROI), the RNA transcripts within ROI are spatially crosslinked to the barcodes. One benefit of this light-directed method is that it allows researcher to actively select the region for barcoding. In addition, it can cover all types of RNA instead of the only mRNA because barcode crosslinking is light-directed instead of poly-(dT) hybridization. Furthermore, instead of digesting the sample, light-seq releases their cDNA in a nondestructive way, equipping it with the potential compatibility for multi-omic studies (such as protein and lipid detection). In a proof-of-principle study, Light-seq has successfully selected and profiled eight rare dopaminergic amacrine cell subtypes from a large tissue sample and discovered new RNA biomarkers for them.<sup>83</sup> Further improvement can be made in future development regarding its barcoding stringency and efficiency, which are currently bottle-necked by the photo-crosslinking efficiency and the effectiveness of washing away barcodes from the previous round.

GeoMx<sup>84</sup> is the commercially available spatial transcriptomics technique for *in situ* barcoding followed by *ex situ* sequencing. ISH probes linked to DNA barcodes by a photocleavable linker are added onto the slide where the sample is mounted and hybridized to the RNA targets. The barcodes are spatially released by UV-illumination on the ROIs, indexed to ROIs, and sequenced. Barcodes and ROI indices are combined to reveal the spatial location of every RNA. This is a highly standardized protocol, making it easy for researchers to use. Similar to light-seq, it benefits from the nondestructive barcoding scheme, giving it potential to combine with multi-omic studies. It also equips researchers with flexible manipulation on the tissue because it allows user-determined ROI selections. Though in comparison to DBiT-seq and Light-seq which enable untargeted spatial transcriptomics analysis, GeoMx requires the prior knowledge of the RNA sequences to predesign DNA-barcoded ISH probes.

To summarize, the past two decades have seen a rapid growth of spatial transcriptomics techniques through many novel designs and implementations, as we have covered in this section. Each option in the wide selection of spatial transcriptomics techniques offers unique capabilities that help unravel previously inaccessible biological systems. In the following section, we will elaborate some typical examples, categorized across different spatial resolutions—from subcellular to whole tissue level.

## Spatial Transcriptomics: Applications

### Subcellular level

Spatial information of RNA transcripts on a subcellular level can be used to infer many aspects of the cellular mechanisms (Fig. 2A). Studies have found that RNA transcripts, including both coding and noncoding RNAs,<sup>85</sup> are differentially distributed in the cell. For example, a study using FISSEQ to spatially sequence the transcriptome in human fibroblasts *in situ* has found that noncoding and antisense RNA are more likely to be nuclear, whereas coding mRNAs localize to the cytoplasm.<sup>86</sup> Similarly, MERFISH combined with endoplasmic reticulum (ER) immunolabeling identified gene transcripts that are specifically

enriched in the ER.<sup>63</sup> This study also confirmed that RNA species preferentially enriched in the nucleus include intron-retaining transcripts and long noncoding RNAs (lncRNAs), such as *MALAT1*. These intracellular localization of RNA transcripts has also implied their functional role in regulating gene expression.<sup>34,35</sup> Interestingly, hundreds of mature protein coding RNAs were also identified in the nucleus, which points to previous studies that suggested this retention of mRNA being a mechanism for buffering cytoplasm gene expression noise.<sup>87,88</sup>

Aside from RNA intracellular localizations, temporal information can also be included to help uncover RNA dynamics.<sup>63,89</sup> For instance, TEMPOMap (temporally resolved *in situ* sequencing and mapping) combines pulse-chase metabolic labeling with multiplexed 3D *in situ* sequencing to investigate subcellular RNA dynamics spatiotemporally.<sup>37</sup> The study confirmed a previous finding that there is a drastic RNA eviction from the chromosomes in M phase cells.<sup>90</sup> Moreover, TEMPOMap provided deeper insight and refinement on the previously proposed RNA velocity model,<sup>36</sup> which described the combined kinetics of RNA synthesis, nuclear export, translocation, and degradation.

In addition, other omics to subcellular spatial transcriptomics can be included, such as proteomics. Protein fluorescent labeling and its colocalization with RNA signals provide further information on cellular mechanisms. One example is regarding translation regulation. For instance, the cellular landmark micro-tubule organizing center (MTOC) indicates polarity in most polarized cells and is often positioned between the nucleus and the leading edges of cells before growth or migration.<sup>91,92</sup> Dyp-FISH, a clustering method for mRNA and protein, discovered the enrichment of total cytoplasmic mRNA transcripts in the MTOC-containing region in polarized fibroblasts.<sup>89</sup> These studies confirm that spatially and temporally restricted translation, that is, local translation, is important for controlling gene expression and protein subcellular localization.<sup>93</sup> Another example is regarding RNA splicing regulation. Co-staining between the nuclear speckle marker SC35 and transcripts of a synthetic spliceable *RG6* minigene revealed that splicing efficiency is higher within proximity of nuclear speckles.<sup>94</sup> Altogether these examples demonstrated that spatial transcriptomics is an essential tool at the subcellular resolution and provides valuable information in RNA mechanisms, dynamics, and so on.

## Cellular level

Many spatial transcriptomics techniques are well positioned on a cellular level (Table 1) to provide unique resources to study diverse biological processes. We will describe two examples in this section: cell–cell communications (CCC), as well as embryo development and organogenesis.

CCCs are fundamental for tissue organization and function.<sup>95</sup> To investigate CCC, it is important to preserve the cell–cell neighboring information, while monitoring the RNA expression perturbation at the single-cell level. Spatial transcriptomics helps to achieve this goal. One form of CCC is via soluble ligand-receptor pair, where the corresponding changes in mRNA can be detected with cells that are in communication (Fig. 2B). Inference methods such as COMMOT<sup>96</sup> and SpaTalk<sup>97</sup> were applied to various spatial transcriptomics datasets

to infer the spatial signaling directionality, as well as the competition and interaction between different ligands and receptor species.

Additionally, spatial transcriptomics helps investigate communication through direct contact (e.g., gap junctions) between immediate neighboring cells. CellNeighborEX was proposed to specifically address gene signatures that are the result of this form of neighbor-dependent expression using transcriptome spatial transcriptomics datasets.<sup>98</sup> This study showed that in various tissues, cells exhibit differential expression profiles based on the cell types they are neighboring. In particular, CellNeighborEX identified development-associated genes in embryos and metastases-associated genes in liver cancer tissue that showed neighbor-dependent expressions. More generally, unbiased methods such as the node-centric expression models have been proposed to consider the effect of cell niche composition on global gene signatures.<sup>99</sup> This method can be applied to high-resolution spatial transcriptomics techniques such as MERFISH, as well as spot-based approaches such as Visium and Slide-seq, provided that deconvolution analyses are able to recover within-cell-type variation for these datasets. Additional computational methods for inferring CCC from spatial transcriptomics data were reviewed previously.<sup>100</sup>

Spatial transcriptomics on single-cell level has also been used to study embryo development and organogenesis (Fig. 2B). In addition to the transcriptome information provided by scRNA-seq, spatial transcriptomics provide directionality context in embryo studies and help identify genes with anatomically patterned expression.<sup>101</sup> For example, Stereo-seq<sup>76</sup> enables large field-of-view spatial transcriptomics on whole mouse embryos, while also achieving cellular resolution. This technology generated the mouse organogenesis spatiotemporal transcriptomic atlas (MOSTA), which not only maps the spatial cell heterogeneity in mouse embryo tissues but also captures transcriptome trajectory in organogenesis. Additionally, the ability of Stereo-seq to capture intronic transcripts enables calculation of RNA velocity on single-cell level, thus facilitating investigations of cell fate transitions.

While similar studies<sup>102–104</sup> demonstrated the immense potential of single-cell spatial transcriptomics in studying mouse organogenesis, the first application in human was reported recently,<sup>105</sup> where the transcriptional landscape of 4- to 6-week human embryos was spatially mapped. In particular, this work resolved previously uncharacterized structures such as the head mesoderm and profiled undefined cell types. Taken together, these examples demonstrate the versatility of spatial transcriptomics within cellular-level applications.

## Tissue level

Identifying cell types and their positional context in tissues is crucial for understanding tissue normal function and pathological changes (Fig. 2C). Spatial transcriptomics has been used widely in spatially mapping tissues, including the bone marrow,<sup>106</sup> testis,<sup>107</sup> developmental heart,<sup>108</sup> and gut.<sup>109</sup> Specifically, spatial transcriptomics has made great strides in profiling mammalian brain, which is one of the most complex structures that contain millions to hundreds of billions of cells with an extremely high order of organization.<sup>110</sup> Collectively, studies demonstrated that spatial transcriptomics can accurately resolve cell types and their proportions in the cerebellum,<sup>71,111,112</sup>

hippocampus,<sup>72,108,111–114</sup> olfactory bulb,<sup>41,114,115</sup> and more.<sup>109,116</sup> In addition to normal brain architecture, pathophysiology changes to the brain have also been characterized with spatial transcriptomics in Alzheimer's disease,<sup>112</sup> schizophrenia,<sup>117</sup> autism,<sup>117</sup> and traumatic brain injury.<sup>71</sup>

Spatial transcriptomics has also been widely applied to study pathological changes in cancer. It is important to characterize tumor cellular compositions, since intratumor transcriptional heterogeneity hugely challenges cancer diagnosis and treatment.<sup>118</sup> Early studies using scRNA-seq finely characterized tumor heterogeneity in their cellular transcriptional programs,<sup>119</sup> with spatial transcriptomics supplementing our understanding of cancer through profiling the differential localization of tumor subpopulations. In addition, the spatial interactions between tumors and surrounding healthy tissues are crucial to characterize. Spatial transcriptomics excelled at advancing this area of research in various types of cancer, including pancreatic ductal adenocarcinoma (PDAC),<sup>113,114,116,120</sup> prostate cancer,<sup>121</sup> melanoma,<sup>116,122</sup> and breast cancer.<sup>116</sup> Specifically, in PDAC tissue architecture, research using spatial transcriptomics have agreed that subpopulations of ductal cells, macrophages, dendritic cells, and cancer cells enrich in a spatially restricted manner. The colocalization between cancer cells and inflammatory fibroblasts were also commonly noted with the aid of spatial transcriptomics.<sup>113,114,116,120</sup>

One integral area of research to tissue spatial transcriptomics application is developing computational tools for data analysis. The rapid development of spatial transcriptomics techniques has brought unprecedented depth to our understanding of the spatial transcriptome. At the same time, novel datasets produced by spatial transcriptomics techniques present challenges in data analysis. To efficiently use the spatial information provided by spatial transcriptomics, computational algorithms have been developed to specifically accommodate spatial transcriptomics data. For example, BayesSpace<sup>123</sup> enhances the resolution of spot-based spatial transcriptomics techniques to subspot level, resolving tissue structures that are not detectable at original resolution. Similarly, SpatialPCA<sup>124</sup> denoises spatial transcriptomics data by extracting low-dimension representations and explicitly modeling the spatial correlation across tissue locations. As a third example, Vesalius<sup>125</sup> recovers tissue territories from high-resolution spatial transcriptomics data through embedding spatial transcriptomics data into RGB arrays and leveraging image analysis techniques. Computational methods tailored to spatial transcriptomics data have been comprehensively reviewed.<sup>126,127</sup>

In summary, spatial transcriptomics techniques have empowered investigations in diverse areas of biology and biomedicine. These examples of fruitful research employed different spatial transcriptomics techniques to specifically address their respective interests. Depending on the research objective, one's selection of spatial transcriptomics method varies because different technologies have their strength and drawbacks, as we reviewed in the sections above. Therefore, for researchers new to spatial transcriptomics, we elaborate in the following section a number of factors to consider when choosing an spatial transcriptomics technique that is best suited for their investigations.



## Factors to consider for choosing spatial transcriptomics methods

When selecting an spatial transcriptomics technique, some key factors that must be considered include but are not limited to detection efficiency, transcriptome coverage, scale of experiment, as well as the required spatial resolution (Table 1). In the following, we will discuss three main aspects in more detail.

First, whether the RNA targets are predefined, plays an important role in determining the choice of spatial transcriptomics techniques, as it highlights the difference between discovery-driven and hypothesis-driven spatial transcriptomics studies. Discovery-driven studies aim to characterize the entire transcriptome in an unbiased manner. *Ex situ* sequencing-based techniques are well-suited for this type of research, as they enable highly parallel profiling of mRNA without prior knowledge of their sequences. Conversely, hypothesis-driven studies often focus on a limited number of known RNA transcripts for in-depth characterization. For this purpose, hybridization-based techniques offer higher detection rates, improved spatial resolution, and the potential for combination with immunostaining. Techniques such as seqFISH,<sup>58</sup> seqFISH+,<sup>62</sup> and MERFISH<sup>42–45</sup> allow for multiplexed characterization of over a thousand RNA transcripts in hypothesis-driven studies. *In situ* sequencing-based techniques can accommodate both discovery- and hypothesis-driven studies due to their ability to sequence RNA in its native context using either targeting or nontargeting primers.<sup>65,58</sup>

Second, the trade-off between detection efficiency and coverage should also be considered. Hybridization-based methods excel in detecting specific subsets of RNA with high efficiency, but the number of RNA sequences that they can detect is limited. These methods are typically preferred for studying RNA transcripts with low abundance, where missing any RNA will largely impact the outcome. In particular, smFISH offers the highest detection efficiency and is best for detecting a handful of RNA sequences. seqFISH+ and MERFISH offer higher transcriptomic coverage, but at the cost of having lower detection efficiency than smFISH. *Ex situ* sequencing-based methods provide extensive coverage of the transcriptome, but their detection efficiency is even lower. For this reason, they are more suitable for transcriptome-wide studies with abundant RNA species.

In addition, the level of spatial resolution should be considered, which is often influenced by the scale of the experiment. For large-scale tissue analyses where only near-cellular resolution is required, *ex situ* sequencing methods are preferred, such as the 10X Visium kit with its 11×11 mm capturing area and high transcriptome throughput. On a finer scale, cellular studies often require higher spatial resolution of RNA, sometimes down to their subcellular localizations (e.g., RNA velocity<sup>36,37</sup>). These studies will benefit more from hybridization-based methods such as smFISH, seqFISH+, and MERFISH that are capable of providing subcellular resolution.

Furthermore, the experimental time and accessibility should be considered. Hybridization-based and *in situ* sequencing-based techniques, though they offer high-spatial resolution, require extensive sample preparation and complicated iterative imaging schemes, which are very time-consuming. The experiment pipelines for these techniques can be highly technical and require extensive training to ensure data quality, which impedes easy access



for academic and clinical uses. On the other hand, commercially available *ex situ* sequencing techniques such as 10X Visium<sup>79</sup> and SlideSeq,<sup>71,73</sup> despite limited spatial resolution, detection efficiency, and coverage, offer standardized sample preparation processes and require shorter time in preparation and are more accessible to academic and clinical researchers.

Lastly, the cost should be considered as well. For example, high-efficiency hybridization-based techniques, such as smFISH, often require a set of more than 20 fluorescent probes per gene, costing roughly \$1000. Multiplexable techniques such as seqFISH+<sup>62</sup> and MERFISH,<sup>42–45</sup> through barcoding and the use of target-independent fluorescent read-out probes, achieve much cheaper relative cost per gene when interrogating the transcriptome with coverage of more than 10,000 genes. In addition, *Ex situ* sequencing-based spatial transcriptomics techniques, such as SlideSeq,<sup>71,73</sup> 10X Visium,<sup>79</sup> and stereo-seq,<sup>76,77</sup> offer kits with different size of capturing areas at different cost. When designing the experiment, researchers should balance their research goals, the size of the sample, and the extent of the transcriptomic coverage to choose these multiplexable or nonmultiplexable techniques or kits wisely to achieve the most cost-efficient experimental designs.

### Perspective

Despite great achievements, current spatial transcriptomics techniques still have a number of limitations. For instance, hybridization-based techniques have limited base-resolution and can only detect longer RNA transcripts because these methods typically require a set of more than 20 probes covering a region of over 500 bases to detect RNA.<sup>38,39</sup> *In situ* sequencing-based techniques, while capable of discriminating single-base differences, have lower detection efficiency and transcriptome coverage.<sup>65–68</sup> *Ex situ* sequencing-based techniques<sup>70–73,76,79</sup> large rely on poly-(dT)-based mRNA capturing, which has lower detection efficiency, especially for short RNA species. Therefore, current spatial transcriptomics techniques primarily focus on the detection of mRNA and long RNA species, while other RNA species such as isoforms with subtle sequence differences<sup>128–130</sup> or short RNA molecules (like miRNA<sup>131–133</sup>) remain largely unexplored. In addition, all three categories of spatial transcriptomics techniques detect RNA only by their sequences. However, RNA undergoes extensive posttranscriptional modifications<sup>134–136</sup> and form diverse structures<sup>137–139</sup> in the cells. These modifications and structures currently remain undistinguished by spatial transcriptomics techniques.

### Conclusion

Over the past decade, spatial transcriptomics has proven invaluable in the field of transcriptomics alongside other staple methods such as scRNA-seq. It is a set of unique integrative tools that provide crucial spatial information on RNA transcripts, which vastly accelerated our understanding on the transcriptome and its changes in many settings, as reviewed in this article. In the meantime, novel designs and technical advancements have made great improvements on throughput, sensitivity, and cost, altogether making spatial transcriptomics accessible to an increasingly wide range of research. We foresee that spatial

transcriptomics will become one of the most important methods in molecular biology and will be pivotal for future transcriptomics studies.

## Funding Information

This work is supported by NIH Director's New Innovator Award (1DP2GM149554).

## References

1. Sharp PA. The centrality of RNA. *Cell* 2009;136(4):577–580; doi: 10.1016/J.CELL.2009.02.007 [PubMed: 19239877]
2. Cooper TA, Wan L, Dreyfuss G. RNA and disease. *Cell* 2009;136(4):777–793; doi: 10.1016/J.CELL.2009.02.011 [PubMed: 19239895]
3. Wang GS, Cooper TA. Splicing in disease: Disruption of the splicing code and the decoding machinery. *Nat Rev Genet* 2007;8(10):749–761; doi: 10.1038/nrg2164 [PubMed: 17726481]
4. Cáceres JF, Kornblihtt AR. Alternative splicing: Multiple control mechanisms and involvement in human disease. *Trends Genet* 2002;18(4):186–193; doi: 10.1016/S0168-9525(01)02626-9 [PubMed: 11932019]
5. Frischmeyer PA, Dietz HC. Nonsense-mediated mRNA decay in health and disease. *Hum Mol Genet* 1999;8(10):1893–1900; doi: 10.1093/HMG/8.10.1893 [PubMed: 10469842]
6. O'Rourke JR, Swanson MS. Mechanisms of RNA-mediated disease. *J Biol Chem* 2009;284(12):7419–7423; doi: 10.1074/JBC.R800025200 [PubMed: 18957432]
7. Lukong KE, Chang K-w, Khandjian EW, et al. RNA-binding proteins in human genetic disease. *Trends Genet* 2008;24(8):416–425; doi: 10.1016/J.TIG.2008.05.004 [PubMed: 18597886]
8. Ponting CP, Oliver PL, Reik W. Evolution and functions of long noncoding RNAs. *Cell* 2009;136(4):629–641; doi: 10.1016/J.CELL.2009.02.006 [PubMed: 19239885]
9. Cech TR, Steitz JA. The noncoding RNA revolution—Trashing old rules to forge new ones. *Cell* 2014;157(1):77–94; doi: 10.1016/J.CELL.2014.03.008 [PubMed: 24679528]
10. Bartel DP. MicroRNAs: Genomics, biogenesis, mechanism, and function. *Cell* 2004;116(2):281–297; doi: 10.1016/S0092-8674(04)00045-5 [PubMed: 14744438]
11. Carthew RW, Sontheimer EJ. Origins and mechanisms of miRNAs and siRNAs. *Cell* 2009;136(4):642–655; doi: 10.1016/J.CELL.2009.01.035 [PubMed: 19239886]
12. Zhou WY, Cai ZR, Liu J, et al. Circular RNA: Metabolism, functions and interactions with proteins. *Mol Cancer* 2020;19(1):1–19; doi: 10.1186/S12943-020-01286-3 [PubMed: 31901224]
13. Long Y, Wang X, Youmans DT, et al. How do lncRNAs regulate transcription? *Sci Adv* 2017;3(9):eaao2110; doi: 10.1126/SCIADV.AAO2110/ASSET/7EBE5DCE-6748-48F1-A3DA-EF8CD648797A/ASSETS/GRAPHIC/AAO2110-F4.JPEG [PubMed: 28959731]
14. Bose R, Ain R. Regulation of transcription by circular RNAs. *Adv Exp Med Biol* 2018;1087:81–94; doi: 10.1007/978-981-13-1426-1\_7 [PubMed: 30259359]
15. Statello L, Guo CJ, Chen LL, et al. Gene regulation by long non-coding RNAs and its biological functions. *Nat Rev Mol Cell Biol* 2020;22(2):96–118; doi: 10.1038/s41580-020-00315-9 [PubMed: 33353982]
16. Chen LL. The expanding regulatory mechanisms and cellular functions of circular RNAs. *Nat Rev Mol Cell Biol* 2020;21(8):475–490; doi: 10.1038/s41580-020-0243-y [PubMed: 32366901]
17. Karakas D, Ozpolat B. The role of lncRNAs in translation. *Noncoding RNA* 2021;7(1):1–14; doi: 10.3390/NCRNA7010016
18. Filipowicz W, Bhattacharyya SN, Sonenberg N. Mechanisms of post-transcriptional regulation by microRNAs: Are the answers in sight? *Nat Rev Genet* 2008;9(2):102–114; doi: 10.1038/nrg2290 [PubMed: 18197166]
19. Piwecka M, Rajewsky N, Rybak-Wolf A. Single-cell and spatial transcriptomics: Deciphering brain complexity in health and disease. *Nat Rev Neurol* 2023;19(6):346–362; doi: 10.1038/s41582-023-00809-y [PubMed: 37198436]

20. Miranda AMA, Janbandhu V, Maatz H, et al. Single-cell transcriptomics for the assessment of cardiac disease. *Nat Rev Cardiol* 2022;20(5):289–308; doi: 10.1038/s41569-022-00805-7 [PubMed: 36539452]
21. Ahsanuddin S, Wu AY. Single-cell transcriptomics of the ocular anterior segment: A comprehensive review. *Eye* 2023;1–17; doi: 10.1038/s41433-023-02539-3
22. Fan J, Slowikowski K, Zhang F. Single-cell transcriptomics in cancer: Computational challenges and opportunities. *Exp Mol Med* 2020;52(9):1452–1465; doi: 10.1038/s12276-020-0422-0 [PubMed: 32929226]
23. Zhang Y, Wang D, Peng M, et al. Single-cell RNA sequencing in cancer research. *J Exp Clin Cancer Res* 2021;40(1):1–17; doi: 10.1186/S13046-021-01874-1 [PubMed: 33390177]
24. Sun G, Li Z, Rong D, et al. Single-cell RNA sequencing in cancer: Applications, advances, and emerging challenges. *Mol Ther Oncolytics* 2021;21:183–206; doi: 10.1016/J.OMTO.2021.04.001 [PubMed: 34027052]
25. Yan L, Yang M, Guo H, et al. Single-cell RNA-Seq profiling of human preimplantation embryos and embryonic stem cells. *Nat Struct Mol Biol* 2013;20(9):1131–1139; doi: 10.1038/nsmb.2660 [PubMed: 23934149]
26. Mittenzweig M, Maysyar Y, Cheng S, et al. A single-embryo, single-cell time-resolved model for mouse gastrulation. *Cell* 2021;184(11):2825–2842.e22; doi: 10.1016/J.CELL.2021.04.004 [PubMed: 33932341]
27. Papalexi E, Satija R. Single-cell RNA sequencing to explore immune cell heterogeneity. *Nat Rev Immunol* 2017;18(1):35–45; doi: 10.1038/nri.2017.76 [PubMed: 28787399]
28. Chen H, Ye F, Guo G. Revolutionizing immunology with single-cell RNA sequencing. *Cell Mol Immunol* 2019;16(3):242–249; doi: 10.1038/s41423-019-0214-4 [PubMed: 30796351]
29. Duran RC-D, Wei H, Wu JQ. Single-cell RNA-sequencing of the brain. *Clin Transl Med* 2017;6(1):20; doi: 10.1186/S40169-017-0150-9 [PubMed: 28597408]
30. Travaglini KJ, Nabhan AN, Penland L, et al. A molecular cell atlas of the human lung from single-cell RNA sequencing. *Nature* 2020;587(7835):619–625; doi: 10.1038/s41586-020-2922-4 [PubMed: 33208946]
31. Paik DT, Cho S, Tian L, et al. Single-cell RNA sequencing in cardiovascular development, disease and medicine. *Nat Rev Cardiol* 2020;17(8):457–473; doi: 10.1038/s41569-020-0359-y [PubMed: 32231331]
32. Marx V Method of the year: Spatially resolved transcriptomics. *Nat Methods* 2021;18(1):9–14; doi: 10.1038/s41592-020-01033-y [PubMed: 33408395]
33. Jin MZ, Jin WL. The updated landscape of tumor microenvironment and drug repurposing. *Signal Transduct Targeted Ther* 2020;5(1):1–16; doi: 10.1038/s41392-020-00280-x
34. Buxbaum AR, Haimovich G, Singer RH. In the right place at the right time: Visualizing and understanding mRNA localization. *Nat Rev Mol Cell Biol* 2014;16(2):95–109; doi: 10.1038/nrm3918 [PubMed: 25549890]
35. Lécuyer E, Yoshida H, Parthasarathy N, et al. Global analysis of mRNA localization reveals a prominent role in organizing cellular architecture and function. *Cell* 2007;131(1):174–187; doi: 10.1016/j.cell.2007.08.003 [PubMed: 17923096]
36. La Manno G, Soldatov R, Zeisel A, et al. RNA velocity of single cells. *Nature* 2018;560(7719):494–498; doi: 10.1038/s41586-018-0414-6 [PubMed: 30089906]
37. Ren J, Zhou H, Zeng H, et al. Spatiotemporally resolved transcriptomics reveals the subcellular RNA kinetic landscape. *Nat Methods* 2023;20(5):1–11; doi: 10.1038/s41592-023-01829-8 [PubMed: 36635552]
38. Raj A, van den Bogaard P, Rifkin SA, et al. Imaging individual mRNA molecules using multiple singly labeled probes. *Nat Methods* 2008;5(10):877–879; doi: 10.1038/nmeth.1253 [PubMed: 18806792]
39. Femino AM, Fay FS, Fogarty K, et al. Visualization of single RNA transcripts in situ. *Science* 1998;280(5363):585–590; doi: 10.1126/science.280.5363.585 [PubMed: 9554849]
40. Goodwin S, McPherson JD, McCombie WR. Coming of age: Ten years of next-generation sequencing technologies. *Nat Rev Genet* 2016;17(6):333–351; doi: 10.1038/nrg.2016.49 [PubMed: 27184599]

41. Ståhl PL, Salmén F, Vickovic S, et al. Visualization and analysis of gene expression in tissue sections by spatial transcriptomics. *Science* 2016;353(6294):78–82; doi: 10.1126/SCIENCE.AAF2403/SUPPL\_FILE/AAF2403\_STAHL\_SM.PDF [PubMed: 27365449]
42. Moffitt JR, Hao J, Wang G, et al. High-throughput single-cell gene-expression profiling with multiplexed error-robust fluorescence in situ hybridization. *Proc Natl Acad Sci U S A* 2016;113(39):11046–11051; doi: 10.1073/PNAS.1612826113/SUPPL\_FILE/PNAS.1612826113.SD01.XLSX [PubMed: 27625426]
43. Moffitt JR, Zhuang X. RNA imaging with multiplexed error robust fluorescence in situ hybridization. *Methods Enzymol* 2016;572:1; doi: 10.1016/BS.MIE.2016.03.020 [PubMed: 27241748]
44. Chen KH, Boettiger AN, Moffitt JR, et al. Spatially resolved, highly multiplexed RNA profiling in single cells. *Science* 2015;348(6233):aaa6090; doi: 10.1126/SCIENCE.AAA6090/SUPPL\_FILE/CHEN-SM.PDF [PubMed: 25858977]
45. Xia C, Babcock HP, Moffitt JR, et al. Multiplexed detection of RNA using MERFISH and branched DNA amplification. *Sci Rep* 2019;9(1):1–13; doi: 10.1038/s41598-019-43943-8 [PubMed: 30626917]
46. Shaffer SM, Wu MT, Levesque MJ, et al. Turbo FISH: A method for rapid single molecule RNA FISH. *PLoS One* 2013;8(9); doi: 10.1371/journal.pone.0075120
47. Levesque MJ, Ginart P, Wei Y, et al. Visualizing SNVs to quantify allele-specific expression in single cells. *Nat Methods* 2013;10(9):865–867; doi: 10.1038/nmeth.2589 [PubMed: 23913259]
48. Mellis IA, Gupte R, Raj A, et al. Visualizing adenosine-to-inosine RNA editing in single mammalian cells. *Nat Methods* 2017;14(8):801–804; doi: 10.1038/nMeth.4332 [PubMed: 28604724]
49. Dirks RM, Pierce NA. Triggered amplification by hybridization chain reaction. *PNAS* 2004;101(43):15275–15278; doi: 10.1073/pnas.0407024101 [PubMed: 15492210]
50. Choi HMT, Beck VA, Pierce NA. Next-generation in situ hybridization chain reaction: Higher gain, lower cost, greater durability. *ACS Nano* 2014;8(5):4284–4294; doi: 10.1021/nn405717p [PubMed: 24712299]
51. Choi HMT, Schwarzkopf M, Fornace ME, et al. Third-generation in situ hybridization chain reaction: Multiplexed, quantitative, sensitive, versatile, robust. *Development* 2018;145(12); doi: 10.1242/dev.165753
52. Moreno-Velásquez SD, Pérez JC. Imaging and quantification of mRNA molecules at single-cell resolution in the human fungal pathogen *Candida albicans*. *mSphere* 2021;6(4):e0041121; doi: 10.1128/mSphere.00411-21 [PubMed: 34232078]
53. Jang MJ, Coughlin GM, Jackson CR, et al. Spatial transcriptomics for profiling the tropism of viral vectors in tissues. *Nat Biotechnol* 2023;41(9):1272–1286; doi: 10.1038/s41587-022-01648-w [PubMed: 36702899]
54. Marras SAE, Bushkin Y, Tyagi S. High-fidelity amplified FISH for the detection and allelic discrimination of single mRNA molecules. *Proc Natl Acad Sci U S A* 2019;116(28):13921–13926; doi: 10.1073/pnas.1814463116 [PubMed: 31221755]
55. Wang F, Flanagan J, Su N, et al. RNAscope: A novel in situ RNA analysis platform for formalin-fixed, paraffin-embedded tissues. *J Mol Diagn* 2012;14(1):22–29; doi: 10.1016/j.jmoldx.2011.08.002 [PubMed: 22166544]
56. Rouhanifard SH, Mellis IA, Dunagin M, et al. ClampFISH detects individual nucleic acid molecules using click chemistry-based amplification. *Nat Biotechnol* 2019;37(1):84–94; doi: 10.1038/nbt.4286
57. Dardani I, Emert BL, Goyal Y, et al. ClampFISH 2.0 enables rapid, scalable amplified RNA detection in situ. *Nat Methods* 2022;19(11):1403–1410; doi: 10.1038/s41592-022-01653-6 [PubMed: 36280724]
58. Lubeck E, Coskun AF, Zhiyentayev T, et al. Single-cell in situ RNA profiling by sequential hybridization. *Nat Methods* 2014;11(4):360–361; doi: 10.1038/nmeth.2892 [PubMed: 24681720]
59. Shah S, Lubeck E, Zhou W, et al. In situ transcription profiling of single cells reveals spatial organization of cells in the mouse hippocampus. *Neuron* 2016;92(2):342–357; doi: 10.1016/j.neuron.2016.10.001 [PubMed: 27764670]

60. Shah S, Lubeck E, Zhou W, et al. seqFISH accurately detects transcripts in single cells and reveals robust spatial organization in the hippocampus. *Neuron* 2017;94(4):752–758.e1; doi: 10.1016/j.neuron.2017.05.008 [PubMed: 28521130]
61. Takei Y, Shah S, Harvey S, et al. Multiplexed dynamic imaging of genomic loci by combined CRISPR imaging and DNA sequential FISH. *Biophys J* 2017;112(9):1773–1776; doi: 10.1016/j.bpj.2017.03.024 [PubMed: 28427715]
62. Eng CHL, Lawson M, Zhu Q, et al. Transcriptome-scale super-resolved imaging in tissues by RNA seqFISH+. *Nature* 2019;568(7751):235–239; doi: 10.1038/s41586-019-1049-y [PubMed: 30911168]
63. Xia C, Fan J, Emanuel G, et al. Spatial transcriptome profiling by MERFISH reveals subcellular RNA compartmentalization and cell cycle-dependent gene expression. *Proc Natl Acad Sci U S A* 2019;116(39):19490–19499; doi: 10.1073/pnas.1912459116 [PubMed: 31501331]
64. Moffitt JR, Hao J, Bambah-Mukku D, et al. High-performance multiplexed fluorescence in situ hybridization in culture and tissue with matrix imprinting and clearing. *Proc Natl Acad Sci U S A* 2016;113(50):14456–14461; doi: 10.1073/pnas.1617699113 [PubMed: 27911841]
65. Lee JH, Daugharthy ER, Scheiman J, et al. Fluorescent in situ sequencing (FISSEQ) of RNA for gene expression profiling in intact cells and tissues. *Nat Protoc* 2015;10(3):442–458; doi: 10.1038/nprot.2014.191 [PubMed: 25675209]
66. Chen X, Sun YC, Church GM, et al. Efficient in situ barcode sequencing using padlock probe-based BaristaSeq. *Nucleic Acids Res* 2018;46(4):e22; doi: 10.1093/nar/gkx1206 [PubMed: 29190363]
67. Wang X, Allen WE, Wright MA, et al. Three-dimensional intact-tissue sequencing of single-cell transcriptional states. *Science* 2018;361(6400):eaat5691; doi: 10.1126/science.aat5691 [PubMed: 29930089]
68. Alon S, Goodwin DR, Sinha A, et al. Expansion sequencing: Spatially precise in situ transcriptomics in intact biological systems. *Science* 2021;371(6528):eaax2656; doi: 10.1126/science.aax2656 [PubMed: 33509999]
69. Chung K, Wallace J, Kim S-Y, et al. Structural and molecular interrogation of intact biological systems. *Nature* 2013;497(7449):332–337; doi: 10.1038/nature12107 [PubMed: 23575631]
70. Lee Y, Bogdanoff D, Wang Y, et al. XYZeq: Spatially resolved single-cell RNA sequencing reveals expression heterogeneity in the tumor micro-environment. *Sci Adv* 2021;7(17):eabg4755; doi: 10.1126/SCIADV.ABG4755 [PubMed: 33883145]
71. Rodriques SG, Stickels RR, Goeva A, et al. Slide-seq: A scalable technology for measuring genome-wide expression at high spatial resolution. *Science* 2019;363(6434):1463–1467; doi: 10.1126/science.aaw1219 [PubMed: 30923225]
72. Vickovic S, Eraslan G, Salmén F, et al. High-definition spatial transcriptomics for in situ tissue profiling. *Nat Methods* 2019;16(10):987–990; doi: 10.1038/s41592-019-0548-y [PubMed: 31501547]
73. Stickels RR, Murray E, Kumar P, et al. Highly sensitive spatial transcriptomics at near-cellular resolution with Slide-seqV2. *Nat Biotechnol* 2021;39(3):313–319; doi: 10.1038/s41587-020-0739-1 [PubMed: 33288904]
74. Bioscience Curio. Curio Seeker: High Resolution Spatial Mapping. 2023. Available from: <https://Curiobioscience.Com/Product/> [Last accessed: September 28, 2023].
75. Mantri M, Hinchman MM, McKellar DW, et al. Spatiotemporal transcriptomics reveals pathogenesis of viral myocarditis. *Nat Cardiovasc Res* 2022;1(10):946–960; doi: 10.1038/s44161-022-00138-1 [PubMed: 36970396]
76. Chen A, Liao S, Cheng M, et al. Spatiotemporal transcriptomic atlas of mouse organogenesis using DNA nanoball-patterned arrays. *Cell* 2022;185(10):1777–1792.e21; doi: 10.1016/j.cell.2022.04.003 [PubMed: 35512705]
77. STOmics. Stereo-Seq Transcriptomics Solution. 2023. Available from: <https://en.stomics.tech/> [Last accessed: September 28, 2023].
78. Wei X, Fu S, Li H, et al. Single-cell Stereo-seq reveals induced progenitor cells involved in axolotl brain regeneration. *Science* 2022;377(6610); doi: 10.1126/science.abp9444



79. 10X Genomics. Map the Whole Transcriptome within the Tissue Context. 2023. Available from: <https://www.10xgenomics.com/platforms/visium> [Last accessed: September 28, 2023].
80. Zhao T, Chiang ZD, Morriss JW, et al. Spatial genomics enables multi-modal study of clonal heterogeneity in tissues. *Nature* 2022;601(7891):85–91; doi: 10.1038/s41586-021-04217-4 [PubMed: 34912115]
81. Liu Y, Yang M, Deng Y, et al. High-spatial-resolution multi-omics sequencing via deterministic barcoding in tissue. *Cell* 2020;183(6):1665–1681.e18; doi: 10.1016/j.cell.2020.10.026 [PubMed: 33188776]
82. Zhang D, Deng Y, Kukanja P, et al. Spatial epigenome–transcriptome co-profiling of mammalian tissues. *Nature* 2023;616(7955):113–122; doi: 10.1038/s41586-023-05795-1 [PubMed: 36922587]
83. Kishi JY, Liu N, West ER, et al. Light-Seq: Light-directed in situ barcoding of biomolecules in fixed cells and tissues for spatially indexed sequencing. *Nat Methods* 2022;19(11):1393–1402; doi: 10.1038/s41592-022-01604-1 [PubMed: 36216958]
84. NanoString. GeoMx Digital Spatial Profiler. 2023. Available from: <https://nanosttring.com/products/geomx-digital-spatial-profiler/geomx-dsp-overview/> [Last accessed: September 28, 2023].
85. Engreitz JM, Ollikainen N, Guttman M. Long non-coding RNAs: Spatial amplifiers that control nuclear structure and gene expression. *Nat Rev Mol Cell Biol* 2016;17(12):756–770; doi: 10.1038/nrm.2016.126 [PubMed: 27780979]
86. Lee JH, Daugharthy ER, Scheiman J, et al. Highly multiplexed subcellular RNA sequencing in situ. *Science* 2014;343(6177):1360–1363; doi: 10.1126/SCIENCE.1250212/SUPPL\_FILE/LEE.SM.PDF [PubMed: 24578530]
87. Battich N, Stoeger T, Pelkmans L. Control of transcript variability in single mammalian cells. *Cell* 2015;163(7):1596–1610; doi: 10.1016/J.CELL.2015.11.018 [PubMed: 26687353]
88. Bahar Halpern K, Caspi I, Lemze D, et al. Nuclear retention of mRNA in mammalian tissues. *Cell Rep* 2015;13(12):2653–2662; doi: 10.1016/J.CELREP.2015.11.036 [PubMed: 26711333]
89. Savulescu AF, Brackin R, Bouilhol E, et al. Interrogating RNA and protein spatial subcellular distribution in smFISH data with DypFISH. *Cell Rep Methods* 2021;1(5):100068; doi: 10.1016/j.crmeth.2021.100068 [PubMed: 35474672]
90. Tanenbaum ME, Stern-Ginossar N, Weissman JS, et al. Regulation of mRNA translation during mitosis. *Elife* 2015;4:e07957; doi: 10.7554/ELIFE.07957 [PubMed: 26305499]
91. Hale CM, Chen WC, Khatau SB, et al. SMRT analysis of MTOC and nuclear positioning reveals the role of EB1 and LIC1 in single-cell polarization. *J Cell Sci* 2011;124(24):4267–4285; doi: 10.1242/JCS.091231 [PubMed: 22193958]
92. Gomes ER, Jani S, Gundersen GG. Nuclear movement regulated by Cdc42, MRCK, myosin, and actin flow establishes MTOC polarization in migrating cells. *Cell* 2005;121(3):451–463; doi: 10.1016/J.CELL.2005.02.022 [PubMed: 15882626]
93. Besse F, Ephrussi A. Translational control of localized mRNAs: Restricting protein synthesis in space and time. *Nat Rev Mol Cell Biol* 2008;9(12):971–980; doi: 10.1038/nrm2548 [PubMed: 19023284]
94. Ding F, Elowitz MB. Constitutive splicing and economies of scale in gene expression. *Nat Struct Mol Biol* 2019;26(6):424; doi: 10.1038/S41594-019-0226-X [PubMed: 31133700]
95. Armingol E, Officer A, Harismendy O, et al. Deciphering cell–cell interactions and communication from gene expression. *Nat Rev Genet* 2020;22(2):71–88; doi: 10.1038/s41576-020-00292-x [PubMed: 33168968]
96. Cang Z, Zhao Y, Almet AA, et al. Screening cell–cell communication in spatial transcriptomics via collective optimal transport. *Nat Methods* 2023;20(2):218–228; doi: 10.1038/s41592-022-01728-4 [PubMed: 36690742]
97. Shao X, Li C, Yang H, et al. Knowledge-graph-based cell-cell communication inference for spatially resolved transcriptomic data with SpaTalk. *Nat Commun* 2022;13(1):1–15; doi: 10.1038/s41467-022-32111-8 [PubMed: 34983933]
98. Kim H, Lövkvist C, Palma AM, et al. CellNeighborEX: Deciphering neighbor-dependent gene expression from spatial transcriptomics data. *bioRxiv* 2023;2022.02.16.480673; doi: 10.1101/2022.02.16.480673

99. Fischer DS, Schaar AC, Theis FJ. Modeling intercellular communication in tissues using spatial graphs of cells. *Nat Biotechnol* 2022;41(3):332–336; doi: 10.1038/s41587-022-01467-z [PubMed: 36302986]
100. Almet AA, Cang Z, Jin S, et al. The landscape of cell–cell communication through single-cell transcriptomics. *Curr Opin Syst Biol* 2021;26:12–23; doi: 10.1016/J.COISB.2021.03.007 [PubMed: 33969247]
101. Waylen LN, Nim HT, Martelotto LG, et al. From whole-mount to single-cell spatial assessment of gene expression in 3D. *Commun Biol* 2020;3(1):1–11; doi: 10.1038/s42003-020-01341-1 [PubMed: 31925316]
102. Peng G, Suo S, Cui G, et al. Molecular architecture of lineage allocation and tissue organization in early mouse embryo. *Nature* 2019;572(7770):528–532; doi: 10.1038/s41586-019-1469-8 [PubMed: 31391582]
103. Lohoff T, Ghazanfar S, Missarova A, et al. Integration of spatial and single-cell transcriptomic data elucidates mouse organogenesis. *Nat Biotechnol* 2021;40(1):74–85; doi: 10.1038/s41587-021-01006-2 [PubMed: 34489600]
104. Srivatsan SR, Regier MC, Barkan E, et al. Embryo-scale, single-cell spatial transcriptomics. *Science* 2021;373(6550):111–117; doi: 10.1126/SCIENCE.ABB9536/SUPPL\_FILE/ABB9536-SRIVATSAN-SM.PDF [PubMed: 34210887]
105. Xu Y, Zhang T, Zhou Q, et al. A single-cell transcriptome atlas profiles early organogenesis in human embryos. *Nat Cell Biol* 2023;25(4):604–615; doi: 10.1038/s41556-023-01108-w [PubMed: 36928764]
106. Baccin C, Al-Sabah J, Velten L, et al. Combined single-cell and spatial transcriptomics reveal the molecular, cellular and spatial bone marrow niche organization. *Nat Cell Biol* 2019;22(1):38–48; doi: 10.1038/s41556-019-0439-6 [PubMed: 31871321]
107. Chen H, Murray E, Sinha A, et al. Dissecting mammalian spermatogenesis using spatial transcriptomics. *Cell Rep* 2021;37(5):109915; doi: 10.1016/J.CELREP.2021.109915 [PubMed: 34731600]
108. Andersson A, Bergenstråhle J, Asp M, et al. Single-cell and spatial transcriptomics enables probabilistic inference of cell type topography. *Commun Biol* 2020;3(1):1–8; doi: 10.1038/s42003-020-01247-y [PubMed: 31925316]
109. Kleshchevnikov V, Shmatko A, Dann E, et al. Cell2location maps fine-grained cell types in spatial transcriptomics. *Nat Biotechnol* 2022;40(5):661–671; doi: 10.1038/s41587-021-01139-4 [PubMed: 35027729]
110. Herculano-Houzel S, Catania K, Manger PR, et al. Mammalian brains are made of these: A dataset of the numbers and densities of neuronal and nonneuronal cells in the Brain of Glires, Primates, Scandentia, Eulipotyphlans, Afrotherians and Artiodactyls, and their relationship with body mass. *Brain Behav Evol* 2015;86(3–4):145–163; doi: 10.1159/000437413 [PubMed: 26418466]
111. Cable DM, Murray E, Zou LS, et al. Robust decomposition of cell type mixtures in spatial transcriptomics. *Nat Biotechnol* 2021;40(4):517–526; doi: 10.1038/s41587-021-00830-w [PubMed: 33603203]
112. Cable DM, Murray E, Shanmugam V, et al. Cell type-specific inference of differential expression in spatial transcriptomics. *Nat Methods* 2022;19(9):1076–1087; doi: 10.1038/s41592-022-01575-3 [PubMed: 36050488]
113. Elosua-Bayes M, Nieto P, Mereu E, et al. SPOTlight: Seeded NMF regression to deconvolute spatial transcriptomics spots with single-cell transcriptomes. *Nucleic Acids Res* 2021;49(9):e50–e50; doi: 10.1093/NAR/GKAB043 [PubMed: 33544846]
114. Ma Y, Zhou X. Spatially informed cell-type deconvolution for spatial transcriptomics. *Nat Biotechnol* 2022;40(9):1349–1359; doi: 10.1038/s41587-022-01273-7 [PubMed: 35501392]
115. Grisanti Canozo FJ, Zuo Z, Martin JF, et al. Cell-type modeling in spatial transcriptomics data elucidates spatially variable colocalization and communication between cell-types in mouse brain. *Cell Syst* 2022;13(1):58–70.e5; doi: 10.1016/J.CELS.2021.09.004 [PubMed: 34626538]



116. Coleman K, Hu J, Schroeder A, et al. SpaDecon: Cell-type deconvolution in spatial transcriptomics with semi-supervised learning. *Comm Biol* 2023;6(1):1–13; doi: 10.1038/s42003-023-04761-x
117. Maynard KR, Collado-Torres L, Weber LM, et al. Transcriptome-scale spatial gene expression in the human dorsolateral prefrontal cortex. *Nat Neurosci* 2021;24(3):425–436; doi: 10.1038/s41593-020-00787-0 [PubMed: 33558695]
118. Bedard PL, Hansen AR, Ratain MJ, et al. Tumour heterogeneity in the clinic. *Nature* 2013;501(7467):355–364; doi: 10.1038/nature12627 [PubMed: 24048068]
119. González-Silva L, Quevedo L, Varela I. Tumor functional heterogeneity unraveled by scRNA-seq technologies. *Trends Cancer* 2020;6(1):13–19; doi: 10.1016/j.trecan.2019.11.010 [PubMed: 31952776]
120. Moncada R, Barkley D, Wagner F, et al. Integrating microarray-based spatial transcriptomics and single-cell RNA-seq reveals tissue architecture in pancreatic ductal adenocarcinomas. *Nat Biotechnol* 2020;38(3):333–342; doi: 10.1038/s41587-019-0392-8 [PubMed: 31932730]
121. Berglund E, Maaskola J, Schultz N, et al. Spatial maps of prostate cancer transcriptomes reveal an unexplored landscape of heterogeneity. *Nat Commun* 2018;9(1):1–13; doi: 10.1038/s41467-018-04724-5 [PubMed: 29317637]
122. Thrane K, Eriksson H, Maaskola J, et al. Spatially resolved transcriptomics enables dissection of genetic heterogeneity in stage III cutaneous malignant melanoma. *Cancer Res* 2018;78(20):5970–5979; doi: 10.1158/0008-5472.CAN-18-0747/653582/AM/SPATIALLY-RESOLVED-TRANSCRIPTOMICS-ENABLES [PubMed: 30154148]
123. Zhao E, Stone MR, Ren X, et al. Spatial transcriptomics at subspot resolution with BayesSpace. *Nat Biotechnol* 2021;39(11):1375–1384; doi: 10.1038/s41587-021-00935-2 [PubMed: 34083791]
124. Shang L, Zhou X. Spatially aware dimension reduction for spatial transcriptomics. *Nat Commun* 2022;13(1):1–22; doi: 10.1038/s41467-022-34879-1 [PubMed: 34983933]
125. Martin PCN, Kim H, Lövkvist C, et al. Vesalius: High-resolution in silico anatomization of spatial transcriptomic data using image analysis. *Mol Syst Biol* 2022;18(9):e11080; doi: 10.15252/MSB.202211080 [PubMed: 36065846]
126. Zeng Z, Li Y, Li Y, et al. Statistical and machine learning methods for spatially resolved transcriptomics data analysis. *Genome Biol* 2022;23(1):1–23; doi: 10.1186/S13059-022-02653-7/FIGURES/3 [PubMed: 34980209]
127. Fang S, Chen B, Zhang Y, et al. Computational approaches and challenges in spatial transcriptomics. *Genomics Proteomics Bioinformatics* 2023;21(1):24–47; doi: 10.1016/J.GPB.2022.10.001 [PubMed: 36252814]
128. Wang ET, Sandberg R, Luo S, et al. Alternative isoform regulation in human tissue transcriptomes. *Nature* 2008;456(7221):470–476; doi: 10.1038/nature07509 [PubMed: 18978772]
129. Ray TA, Cochran K, Kozlowski C, et al. Comprehensive identification of mRNA isoforms reveals the diversity of neural cell-surface molecules with roles in retinal development and disease. *Nat Commun* 2020;11(1):3328; doi: 10.1038/s41467-020-17009-7 [PubMed: 32620864]
130. Lerch JK, Bixby JL, Lemmon VP. Isoform diversity and its importance for axon regeneration. *Neuropathology* 2012;32(4):420–431; doi: 10.1111/j.1440-1789.2011.01280.x [PubMed: 22151581]
131. Guo Z, Maki M, Ding R, et al. Genome-wide survey of tissue-specific micro-RNA and transcription factor regulatory networks in 12 tissues. *Sci Rep* 2014;4(1):5150; doi: 10.1038/srep05150 [PubMed: 24889152]
132. Bayraktar R, Van Roosbroeck K, Calin GA. Cell-to-cell communication: MicroRNAs as hormones. *Mol Oncol* 2017;11(12):1673–1686; doi: 10.1002/1878-0261.12144 [PubMed: 29024380]
133. Gross N, Kropp J, Khatib H. MicroRNA signaling in embryo development. *Biology (Basel)* 2017;6(4):34; doi: 10.3390/biology6030034 [PubMed: 28906477]
134. Wilkinson E, Cui Y-H, He Y-Y. Roles of RNA modifications in diverse cellular functions. *Front Cell Dev Biol* 2022;10; doi: 10.3389/fcell.2022.82868.

135. Barbieri I, Kouzarides T. Role of RNA modifications in cancer. *Nat Rev Cancer* 2020;20(6):303–322; doi: 10.1038/s41568-020-0253-2 [PubMed: 32300195]
136. Cui L, Ma R, Cai J, et al. RNA modifications: Importance in immune cell biology and related diseases. *Signal Transduct Target Ther* 2022;7(1):334; doi: 10.1038/s41392-022-01175-9 [PubMed: 36138023]
137. Ganser LR, Kelly ML, Herschlag D, et al. The roles of structural dynamics in the cellular functions of RNAs. *Nat Rev Mol Cell Biol* 2019;20(8):474–489; doi: 10.1038/s41580-019-0136-0 [PubMed: 31182864]
138. Sun L, Fazal FM, Li P, et al. RNA structure maps across mammalian cellular compartments. *Nat Struct Mol Biol* 2019;26(4):322–330; doi: 10.1038/s41594-019-0200-7 [PubMed: 30886404]
139. Wang J, Zhang T, Yu Z, et al. Genome-wide RNA structure changes during human neurogenesis modulate gene regulatory networks. *Mol Cell* 2021;81(23):4942–4953.e8; doi: 10.1016/j.molcel.2021.09.027 [PubMed: 34655516]

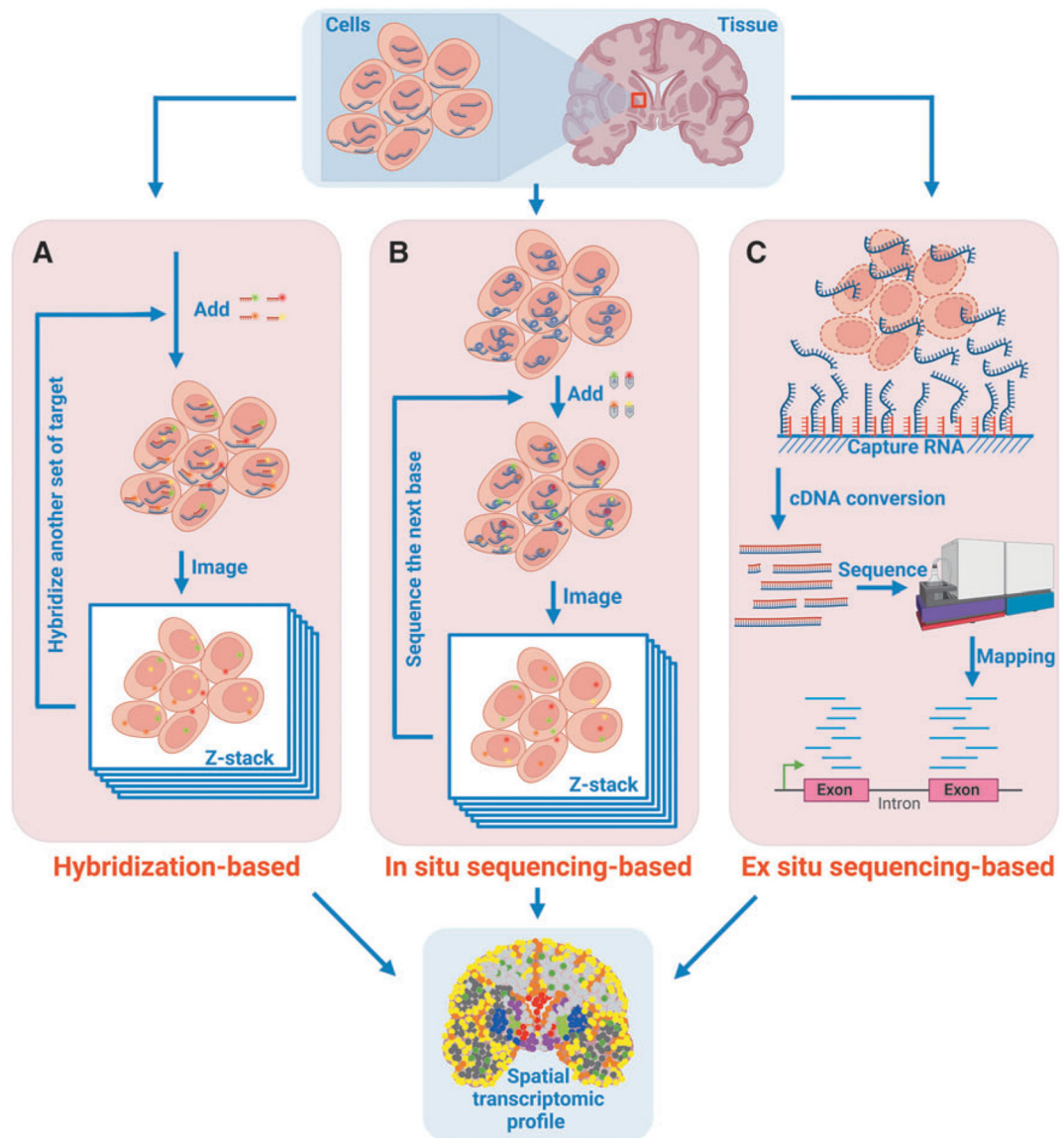


**FIG. 1. Three categories of spatial transcriptomics techniques applied in both cell and tissue samples.**

**(A)** Hybridization-based techniques. To map RNA molecules, DNA probes are pre-labeled with fluorophores and designed with complementary sequences to RNA targets. These fluorescent probes are then added and hybridized to RNA targets inside cells or tissues, with fluorescence signals indicating the location of each target RNA molecule. These techniques are multiplexable, where hybridized probes can be washed away, then new probes are added to identify another set of RNA targets. Depending on the depth/thickness of the sample, Z-direction stack-imaging is required.

**(B)** In situ sequencing-based techniques. In comparison to the hybridization-based methods, sequencing-based platforms add DNA probes as a set of primers to convert RNA targets to cDNA. Then, the cDNA products are circularized *in situ* as templates for rolling-circle amplification to create amplicons in cells or tissues, mimicking the sequencing sample amplicon preparation step in the next-generation sequencing protocols. Then, fluorescent

oligonucleotides or nucleotides are added repetitively and iteratively<sup>79</sup> to perform *in situ* sequencing on the cDNA amplicons. Z-direction stack-imaging is also required to collect all the fluorescent signals.

(C) *Ex situ* sequencing-based techniques. To capture RNA, a capturing slide coated with oligonucleotides that are complementary to RNA are spatially barcoded. The tissue sample is digested on such a capturing slide. After digestion, RNA molecules are released from the sample and are hybridized to the spatially barcoded oligonucleotides. cDNA is synthesized from the captured RNA molecules. The cDNA is amplified, pooled, and sequenced. Then, the sequencing reads are mapped to the transcriptome to identify the RNA identities, and the spatial barcode sequences are used to map the RNA molecules back to their original spatial location on the capturing slide. Data from either (A), (B), or (C) is analyzed and reconstructed into ST profiles. Figure created with ([BioRender.com](https://BioRender.com)). ST, spatial transcriptomics.

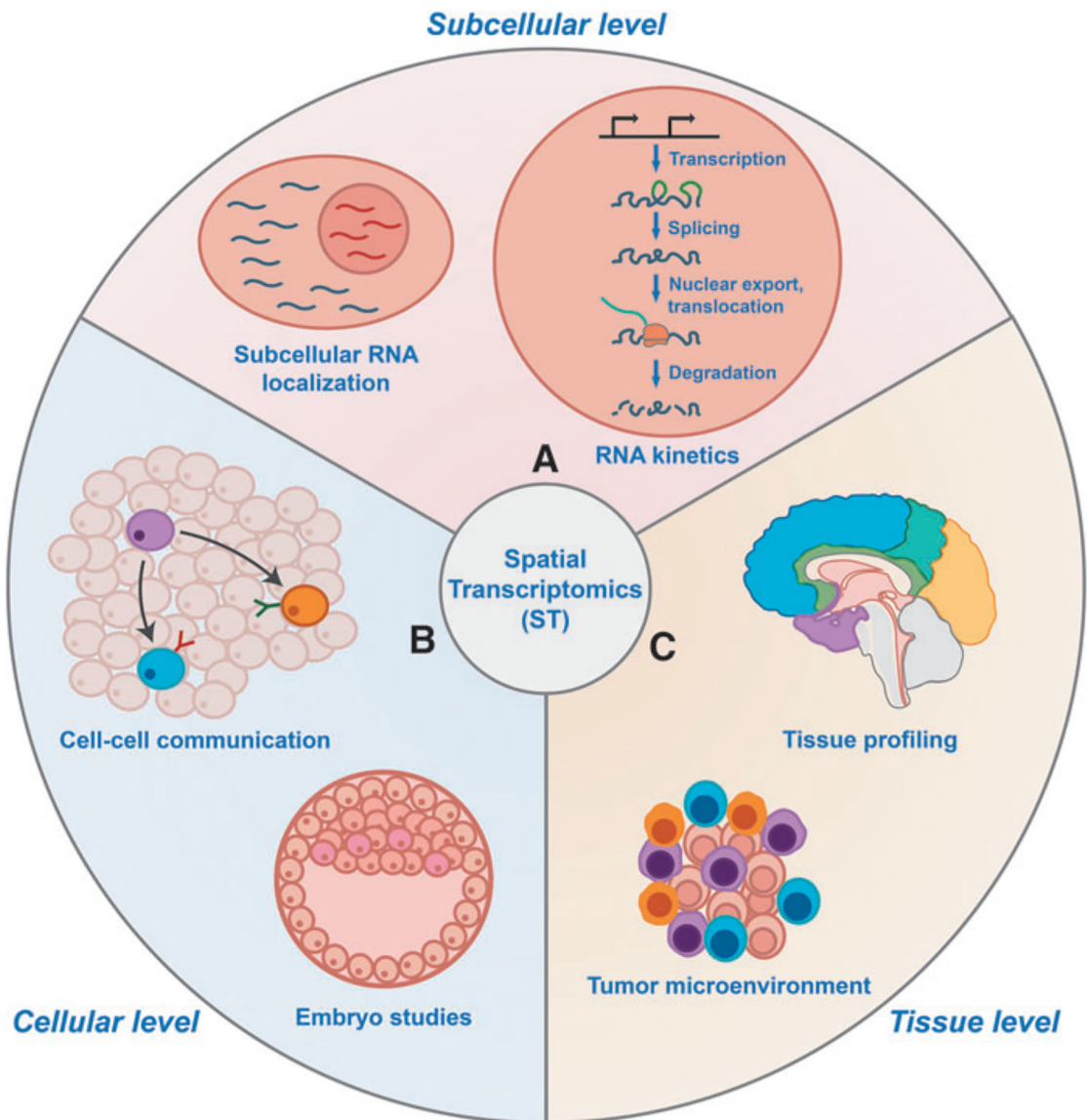


**FIG. 2. Applications of spatial transcriptomics in biological research.**

ST is being rapidly adopted by researchers with diverse interests. This review categorizes the application of ST based on the spatial resolution achieved in the study, then details specific fields of research underneath each resolution level.

(A) At the subcellular level, ST can be used to investigate the localization of RNA transcripts and their functional relationship to cellular structures. In addition, RNA kinetics can be inferred from temporal implementations of ST.

(B) The relative position from cell to cell is vital for their function. Single-cell ST can decipher cell–cell communication through corresponding transcriptome changes while maintaining the neighboring information. The ability to identify different expression programs with positional context is also suitable for studying cell lineage and transcriptome trajectory in early embryos.

(C) On the tissue level, ST profiles cell populations in complex tissue architecture such as the brain. It is also beneficial in cancer biology, where intratumoral cell heterogeneity plays an important role in tumor development and therapeutic resistance. ST, spatial transcriptomics.

Author Manuscript

Author Manuscript

Author Manuscript

Author Manuscript

Table 1.

Spatial transcriptomics techniques and their parameters

	Hybridization-based	Aim	Resolution	Scale	Specificity	Signal-to-noise	Detection efficiency	Transcriptome coverage
	smFISH <sup>38,39</sup>	Mapping single RNA molecules	Single molecule	Subcell, cell, tissue	High	High	High	Low
	TurboFISH <sup>46</sup>	smFISH with reduced experimental time	Single molecule	Subcell, cell	High	High	High	Low
	amp-FISH <sup>54</sup>	Mapping single nucleotide variant	Subcellular	Cell, tissue	Middle-high	Very high	Low-middle	Low
	Toeholded smFISH <sup>47</sup>		Single molecule	Subcell, cell	High	Low	Low	Low
	inoFISH <sup>48</sup>	Mapping A-to-I base-editing	Single molecule	Subcell, cell	High	Low	Low	Low
	U-seqFISH <sup>53</sup>	Mapping short RNA regions	Subcellular	Cell, tissue	Low-middle	Very very high	Low-middle	Low
	ClampFISH <sup>56,57</sup>	Mapping RNA molecules in large sample with high background	Subcellular	Cell, tissue	Low-middle	Very high	Low-middle	Low
	HCR <sup>49-51</sup>		Subcellular	Cell, tissue	Low-middle	Very high	Low-middle	Low
	RNA Scope <sup>55</sup>		Subcellular	Cell, tissue	Low-middle	Very high	Low-middle	Low
	MERFISH <sup>42-45,63</sup>	ST profiling by barcoded hybridization probes	Single molecule	Subcell, cell, tissue	High	High	Middle-high	High
	seqFISH <sup>58</sup>		Single molecule	Subcell, cell, tissue	High	High	Middle-high	Middle
	seqFISH+ <sup>62</sup>		Single molecule	Subcell, cell, tissue	High	High	Middle-high	High
	In situ sequencing-based	Aim	Resolution	Scale	Read length	Signal-to-noise	Detection efficiency	Transcriptome coverage
	BaristaSeq <sup>66</sup>	ST profiling by <i>in situ</i> next-generation sequencing-based sequencing	Single molecule, Single nucleotide	Subcell, cell, tissue	Short	Medium-high	Low	NA
	ExSeq <sup>68</sup>	ST profiling by <i>in situ</i> ligation-based sequencing	Single molecule, Single nucleotide	Subcell, cell, tissue	Short	High	Middle	Middle
	FISSEQ <sup>65</sup>		Single molecule, Single nucleotide	Subcell, cell	Short	Med	Very low	Low
	STARmap <sup>67</sup>		Single molecule, Single nucleotide	Subcell, cell, tissue	Short	High	Middle	High
	Ex situ sequencing-based	Aim	Resolution	Scale	Read length	Lateral diffusion	Detection efficiency	Transcriptome coverage
	DBIT-seq <sup>81</sup>	ST profiling by spatial RNA capturing <i>in situ</i> barcoding and <i>ex situ</i> sequencing	10 $\mu$ m (1.7 cells)	Cell, tissue	Long	Some	High	High
	GeoMx <sup>84</sup>		~ 1 $\mu$ m ROI regions	Cell, tissue	/	No	NA	High
	Light-Seq <sup>83</sup>		< 2 $\mu$ m ROI regions	Cell, tissue	Long	No	Middle	High



HDST <sup>72</sup>	ST profiling by spatial RNA capturing and <i>ex situ</i> sequencing	2 $\mu$ m	Cell, tissue	Long	Some	Middle	High
SlideSeqV1/V2 <sup>71,73</sup>		10 $\mu$ m	Cell, tissue	Long	Some	Low/middle-high	High
StereoSeq <sup>76</sup>		750 nm	Cell, tissue	Long	Some	High	High
XYZseq <sup>70</sup>		500 $\mu$ m	Tissue	Long	Some	High	High
10X Visium <sup>79</sup>		10 cells	Cell, tissue	Long	NA	NA	High

Multiplexity	Throughput	Optical crowding	Targets predefined	Targetable RNA	Sample preservation	Commercial option
Low	Low	No	Yes	RNA >500 nt	Formaldehyde fixation	Stellaris RNA FISH
Low	Low	No	Yes	RNA >500 nt	Formaldehyde/methanol fixation	NA
Low	Low	High	Yes	RNA >40 nt	Formaldehyde fixation	NA
Low	Low	No	Yes	RNA >500 nt	Formaldehyde/methanol fixation	NA
Low	Low	No	Yes	RNA >500 nt	Formaldehyde/methanol fixation	NA
Low	Middle	High	Yes	RNA >40 nt	Formaldehyde fixation	NA
Low	Middle	High	Yes	RNA >500 nt	Formaldehyde fixation	NA
Low	Middle	High	Yes	RNA >500 nt	Formaldehyde fixation	Molecular Instruments
Low	Middle	High	Yes	RNA >500 nt	Formaldehyde fixation	Advanced Cell Diagnostics
High	High	Low	Yes	RNA >500 nt	Formaldehyde fixation	Vizgen
Middle	Middle	Middle	Yes	RNA >500 nt	Formaldehyde fixation	ELEFLOW
High	High	Low	Yes	RNA >500 nt	Formaldehyde fixation	ELEFLOW

Multiplexity	Throughput	Optical Crowding	Targets predefined	Targetable RNA	Sample preservation	Commercial option
High	Middle-high	High	No	All	Formaldehyde fixation	NA
Middle-high	Middle-high	Middle	No	All	Formaldehyde fixation	NA
Middle-high	Middle-high	High	No	All	Formaldehyde fixation	NA
High	High	Middle	Yes	All	Formaldehyde fixation	NA
/	Throughput	/	Targets predefined	Targetable RNA	Sample preservation	Commercial option
/	High	/	No	Polyadenylated RNA, can be modified to accommodate non-polyadenylated RNA	Cryo-preservation, formaldehyde fixation	NA
/	High	/	Yes	All	Cryo-preservation, fixed frozen, FFPE	NanoString
/	High	/	No	Polyadenylated RNA, can be modified to accommodate non-polyadenylated RNA	Formaldehyde fixation	NA
/	High	/	No	Polyadenylated RNA	Cryo-preservation	NA
/	High	/	No	Polyadenylated RNA	Cryo-preservation	Curio Seeker
/	High	/	No	Polyadenylated RNA	Cryo-preservation	STOmics

/	High	/	No	Polyadenylated RNA	Cryo-preservation, Fixed frozen	NA
/	High	/	No	Polyadenylated RNA	Cryo-preservation, FFPE	10X Genomics

*Aim:* The purpose of the ST technique.

*Resolution:* The minimal distinguishable distance between RNA molecules.

*Scale:* The applicable scale of the ST technique, across subcellular, cell, and tissue levels.

*Specificity:* High specificity means low off-targeting signals; low specificity means high off-targeting signals.

*Read length:* The number of bases that can be sequenced. Short <100 bases; long >100 bases.

*Signal-to-noise:* The signal intensity stands out from the background noise intensity.

*Lateral diffusion:* The extent of RNA diffusing from its original position laterally during the RNA capturing step in *ex situ* sequencing-based ST methods.

*Detection efficiency:* The ratio between detected molecules and total molecules to be detected. Note: The comparison of detection efficiency applies within each ST technique category, but not across all three ST technique categories. Typically, hybridization-based methods have a higher detection efficiency than sequencing methods.

*Transcriptome coverage:* The portion of gene detected by ST technique within the whole transcriptome.

*Multiplexity:* The ability to simultaneously detect multiple genes within the sample. Low refers to the ability to multiplex <10 genes simultaneously; high refers to the ability to multiplex at transcriptomic level, usually >500 genes.

*Throughput:* The capacity at which multiple genes and the speed at which multiple cells or tissue samples can be processed and analyzed to obtain spatial transcriptomic information. Throughput evaluation is based on the techniques' multiplexity and sample processing time and capacity. If a technique is able to analyze the sample at low magnification for larger sample areas, its throughput evaluation increases one level from its multiplexity level. If a technique requires extensive sample processing time, its throughput evaluation decreases one level from its multiplexity level.

*Optical crowding:* The hindrance that impairs the distinguishment of different RNA targets due to the proximal clustering of fluorescent signals from these targets or from the background.

*Target predefined:* The requirement of knowing the targeted RNA sequences to design probes for spatial RNA and transcriptomics mapping.

*Targetable RNA:* The types of RNA molecules that can be mapped by the ST technique.

*Sample preservation:* The methods used to preserve samples.

*Commercial option:* The availability of the ST technique from commercial sources.

FFPE, formalin-fixed paraffin-embedded; NA, not applicable; ROI, region of interest; ST, spatial transcriptomics.